

Published in final edited form as:

*Biochem J.* ; 420(2): 191–199. doi:10.1042/BJ20081588.

## Identification and Characterization of the Lipid Binding Property of GrIR, a Locus of Enterocyte Effacement Regulator

Chacko Jobichen<sup>1</sup>, Aaron Zefrin Fernandis<sup>2</sup>, Adrian Velazquez-Campoy<sup>3</sup>, Ka Yin Leung<sup>1,4</sup>, Yu-Keung Mok<sup>1</sup>, Markus R Wenk<sup>1,2</sup>, and J Sivaraman<sup>1,\*</sup>

<sup>1</sup>Department of Biological Sciences, National University of Singapore, Singapore 117543

<sup>2</sup>Yong Loo Lin School of Medicine, Department of Biochemistry, Centre for Life Sciences, National University of Singapore, Singapore 117456

<sup>3</sup>Institute of Biocomputation and Physics of Complex Systems (BIFI), and Fundacion Aragon I+D (ARAID-BIFI), University of Zaragoza, Zaragoza 50009, Spain

<sup>4</sup>Faculty of Natural and Applied Sciences, Department of Biology, Trinity Western University, Langley, B.C., Canada V2Y 1Y1

### Abstract

Lipocalins are a broad family of proteins identified initially in eukaryotes and more recently in gram-negative bacteria. The functions of lipocalin or lipid binding proteins are often elusive and very diverse. We have recently determined the structure of GrIR which plays a key role in the regulation of locus of enterocyte effacement (LEE) proteins. GrIR adopts a lipocalin-like fold which comprises of eight stranded  $\beta$ -barrel followed by an  $\alpha$ -helix at the C-terminus. GrIR has a highly hydrophobic cavity region and could be a potential transporter of lipophilic molecules. To verify this hypothesis, we carried out structure based analysis on GrIR, determined the structure of lipid-GrIR complex and measured the binding of lipid to recombinant GrIR by isothermal titration calorimetry. In addition, we identified that phosphatidylglycerol and phosphatidylethanolamine are the endogenously bound lipid species of GrIR using electrospray ionization mass spectrometry. Further we have shown that the lipid binding property of GrIR is similar to its closest lipocalin structural homolog  $\beta$ -lactoglobulin. Our studies demonstrate the hitherto unknown lipid binding property of GrIR.

### Keywords

Lipocalins; Lipids; TTSS;  $\beta$ -barrel proteins

### Introduction

*Enterohemorrhagic Escherichia coli* (EHEC) and *enteropathogenic E. coli* (EPEC) are the two pathogenic *E. coli* that are responsible for diseases like diarrhea and hemorrhagic colitis in humans and belong to the family of attaching and effacing (A/E) pathogens. During infection, these pathogens use the type III secretion systems (T3SS) to inject effector proteins into the host cells and hijack the normal host cell function to benefit the bacteria. The components and related proteins of T3SS are encoded by 41 genes, organized in five

© 2009 The Authors

\*Corresponding author. dbsjayar@nus.edu.sg.

**Accession Number:** Coordinates of GrIR lipid complex have been deposited in the Protein Data Bank (<http://www.rcsb.org/pdb>) under accession code 3E3C

major operons named locus of enterocyte effacement 1 (LEE1) through LEE5. GrIR is a regulatory protein which plays a major role in the regulation of LEE proteins through its interaction with GrIA, another key regulator. Previously we have reported the structure of GrIR [1].

Structural analysis of GrIR revealed the presence of a hydrophobic cavity in its  $\beta$ -barrel architecture, a feature most commonly observed in lipocalins. Lipocalins are a widespread family of proteins identified in eukaryotes and in gram-negative bacteria [2, 3]. Lipocalins are the carriers of lipophilic molecules but their functions are often elusive and very diverse [4]. The amino acid sequences of lipocalins are poorly conserved except the most general sequence signature GXW motif at the N-terminus [5, 6, 7]. However, GrIR contains a GXY motif at the N-terminus instead of the highly conserved GXW motif. Lipocalins play important role in cryptic coloration, enzymatic synthesis and pheromone transport; they have also been implicated in immune response regulation and modulation of cell homeostasis [8]. The lipocalin fold comprises of an 8 stranded  $\beta$ -barrel followed by an  $\alpha$ -helix at the C-terminus [9, 6]. Blc is the first bacterial lipocalin structurally characterized from *E. coli* [10]. The most prominent structural feature of the lipocalin fold is the presence of a large cup-shaped cavity within the  $\beta$ -barrel and a loop scaffold at its entrance. The selectivity of lipocalin is determined by the amino acid composition of the cavity and loop scaffold, as well as its overall size and conformation [11]. GrIR shares a very high structural similarity with other well-characterized lipocalins, which prompted us to investigate the lipid binding property of GrIR.

As the continuation of our efforts to understand the structure and function of GrIR, here we report the identification and characterization of the lipid binding property of GrIR. Based on structural analysis combined with literature search, we hypothesize that lysophosphatidic acid (LPA) is likely to be the candidate substrate that interact with the hydrophobic cavity of GrIR. To verify this hypothesis, we have determined the crystal structure of the LPA-GrIR complex and performed isothermal calorimetry experiments with LPA and GrIR. Further we have studied and compared the lipid binding property of GrIR with its lipocalin structural homologs. Subsequently, we have identified the physiologically relevant lipid species for GrIR using a mass spectrometry approach. Our studies demonstrate the lipid binding property of GrIR and identify the physiologically relevant family of lipid species that are recognized by GrIR for its hitherto unknown second function.

## Materials and methods

### Protein purification and Crystallization

Plasmid DNA was transformed into *E. coli* BL21 and the cells were grown in LB medium at 37°C to 0.6 AU at OD<sub>600</sub>. One liter of culture was induced with 100  $\mu$ M IPTG and continued to grow at 20°C overnight. Cells were then harvested by centrifugation and resuspended in 40 ml of lysis buffer (50 mM Tris-HCl, pH 7.5, 0.4 M NaCl, 1 mM EDTA, 10 mM  $\beta$ mercaptoethanol and one tablet of Complete<sup>TM</sup> protease inhibitors (Roche Diagnostics). The protein was purified in three steps, using DEAE-Sepharose (Amersham Pharmacia), NI-NTA (Qiagen) and Gel Filtration (Superdex75) columns, respectively. The His-fusion tag was not cleaved. Drops containing 1  $\mu$ l GrIR lipid complex (4 mg/ml) and 1  $\mu$ l reservoir solution were equilibrated by hanging drop vapor diffusion at 21°C. The best crystals were grown from 25% ethylene glycol, 4% tert-butanol and 4% trifluoroethanol (same condition as the apoprotein) with the protein in 20 mM Tris-HCl, pH 7.5, 200 mM NaCl. Crystals measuring ~0.2 mm in length grew over the course of 3 days, belonged to space group P2<sub>1</sub>2<sub>1</sub>2<sub>1</sub> with a=43.73, b=66.02, c=83.46Å and contained two molecules in the asymmetric unit. The Matthews [12] coefficient is 2.2 Å<sup>3</sup>/Da, giving a solvent content of 45%. The X-ray data collection and refinement statistics were given in Table 1.

## Data collection, structure solution and refinement

Crystals were cryo-protected in the reservoir solution supplemented with 40% ethylene glycol and flash cooled at 100°K. X-ray diffraction data were collected at beam line X29A, Brookhaven National Laboratory using a Quantum-4 CCD detector (ADSC). A total of 180 images were collected at 1.1Å wavelength. All the data sets were processed with HKL2000 [13]. The structure was determined using co-crystallized protein crystals by molecular replacement method using Phaser [14] program in the CCP4 crystallographic suite [15]. Native GrIR model was used to obtain the phasing and the structure was further modeled with CNS [16]. The remaining residues of the molecules were added after several cycles of manual model building using O [17] and followed by refinement using CNS [16]. Finally, 264 well-defined water molecules were added, and refinement was continued until the R-value converged to 0.231 ( $R_{\text{free}} = 0.278$ ) for reflections  $I > \sigma(I)$  to 2.5Å resolution. The model had good stereochemistry, with all residues falling within the allowed regions of the Ramachandran plot (Table 1) analyzed by PROCHECK [18].

## Isothermal titration calorimetry

ITC was performed using a VP ITC (MicroCal). GrIR protein was purified using affinity chromatography and gel filtration in 20 mM Tris-HCl buffer at pH 7.5. The purified protein sample was analyzed using mass spectrometry to confirm that no lipid species are bound to it. Bovine  $\beta$ -lactoglobulin (purchased from Sigma Aldrich) was used without further purification, and dialyzed into 20mM Tris-HCl buffer. All lipid samples were at pH 7.5 in 20 mM Tris-HCl. Titrations were performed by injecting consecutive 5-10  $\mu$ l aliquots of lipid solution (0.9–1.0 mM) into the ITC cell containing GrIR or  $\beta$ -lactoglobulin (0.015 mM) at pH 7.5 in 20 mM Tris-HCl. The ITC data were corrected for the heat of dilution of the titrant by subtracting mixing enthalpies for injections of lipid solution into protein-free buffer. Two to four independent titration experiments were performed at 20°C to determine the binding constant of lipid to GrIR. The ITC data analysis was performed using software developed in our laboratory implemented in Origin 7.0 (OriginLab). Because both proteins GrIR and  $\beta$ -lactoglobulin are homodimeric, the protein dimer was employed as the functional unit. A general model based on the overall binding constants for two ligand binding sites, or the model with two identical cooperative ligand binding sites was used in the data analysis.

## Lipid Extraction

The PBS washed Ni-NTA precipitates extracted with 600  $\mu$ l of ice cold chloroform:methanol (1:2). The tubes were vortexed for 1 min and then transferred to a roller shaker in cold room for 1 h. Following incubation, 300  $\mu$ l of ice cold chloroform was added and the tube was vortexed for 30s. The phase was broken with the addition of 200  $\mu$ l of ice cold water. The lipids were extracted by vortexing for 2 min. The phases were separated by centrifugation at 9000 rpm for 5 min. The lower organic phase was transferred to a fresh tube. To the remaining aqueous phase, 300  $\mu$ l of chloroform was added. The phases were vortexed for 2 min and then separated by centrifugation. The lower re- extracted organic phase was pooled with the initial organic phase. The lipids were dried in a speed vacuum. The dried lipids were stored at –80°C till further analysis. Before analysis the lipids were resuspended in 150  $\mu$ l of chloroform: methanol (1:1).

## Mass Spectrometry Analysis

For general profiling, the lipids were initially separated on XTerra C18 reverse phase column (1 mm  $\times$  150 mm) (Waters Corporation) before entering into the mass spectrometer. Typically, 5  $\mu$ l of sample was injected for analysis. The inlet system consisted of a CapLC auto sampler, and a CapLC pump. Chloroform-methanol 1:1 (v/v) with 15 mM piperidine

was used as the mobile phase for isocratic elution at a flow rate of 10  $\mu\text{l}/\text{min}$ . The column elutes were measured using electrospray ionization mass spectrometry (ESI-MS) through a Micromass Q-ToF micro mass spectrometer (Waters Corporation) operated in the negative ion mode. The capillary voltage and sample cone voltage were maintained at 3.0 kV and 50 V, respectively. The source temperature was 80°C and the nanoflow gas pressure was maintained at 0.7 bar. The mass spectrum was acquired from  $m/z$  00 to 1200 in the negative ion mode with an acquisition time of 25 min; the scan duration was 1.2 s. Individual molecular species were identified using tandem mass spectrometry and the collision energy used ranged from 25 to 80 eV.

Quantification of individual lipid molecular species was performed using multiple reaction monitoring (MRM) with an Applied Biosystems 4000 Q-Trap mass spectrometer. Samples were directly introduced into the mass spectrometry using an Agilent autosampler. Each individual ion dissociation pathway for the lipid species was optimized with regard to collision energy to minimize variations in relative ion abundance due to differences in rates of dissociation. An optimized 15  $\mu\text{l}$  of samples was injected per run per set with chloroform:methanol 1:1 (v/v) as the mobile phase at the flow rate of 200  $\mu\text{l}/\text{min}$ . The run was carried out for 2 min.

## Results

### GrIR has a lipocalin like fold

A search on the coordinates of GrIR (PDB code 2ovs) for structurally similar proteins was performed using the program DALI [19]. This search identified several lipocalins with significant structural similarity to the  $\beta$ -barrel architecture of GrIR. While having poor or no sequence homology, lipocalins are structurally very similar to each other. The BLAST [20] (NCBI) search on the GrIR sequence revealed no significant sequence similarities with other lipocalins that are structurally similar to GrIR (Fig. 1A). Lipocalins possess a structurally conserved C-terminal helix at one side of the eight-stranded  $\beta$ -barrel. In GrIR the C-terminal last 11 residues are not clearly visible in the electron density map and this region is presumably disordered. However based on the sequence analysis and modeling this region is likely to form a two turn helix. We speculate that the C terminal region of GrIR is a flexible region with a minimum of two turn  $\alpha$ -helix. The highest structural similarity is observed between GrIR and the lipid-binding domain of  $\beta$ -lactoglobulin, a core lipocalin, yielding an rmsd of 2.8Å for 92 C $\alpha$  atoms (PDB code 1beb; 15% sequence identity). This is followed by the retinol binding protein (PDB code 1aqb; rmsd=3.3Å for 98 C $\alpha$  atoms; 12.6% sequence identity). In addition, 23 lipocalin-like structures or lipid binding proteins revealed significant structural homology with GrIR (Supplementary Table 1). It is worth mentioning that a T3SS secretin pilot protein from *Shigella flexneri* bound with lipids also shows high structural similarity with GrIR [21] (rmsd of 2.8Å for 77 C $\alpha$  atoms; 16% sequence identity; PDB code 1y9t). All the lipocalins have a hydrophobic cavity through which they bind with lipid molecules. For instance, the folds of lipocalins Blc, the first structurally known bacterial lipocalin [10] and Mxim [21] are identical to each other and very similar to GrIR. These observations suggest that the  $\beta$ -barrel architecture is an evolutionarily conserved structural feature for the lipocalins or lipid binding proteins, while at the same time the amino acid sequence of these proteins has diverged to acquire different lipid specificities for their functional roles (Fig. 1B). Based on the size, hydrophobic nature of the  $\beta$ -barrel cavity and structural similarity with other lipocalins, three lipid molecules were identified to interact with GrIR. The lipid molecules which are likely to interact with GrIR are (1) 1, 2-dioctanoyl-*sn*-glycero-3-phosphate, (2) 1-hexanoyl-2-hydroxy-*sn*-glycero-3-phosphate (HHGP) and (3) 1-palmitoyl-2-hydroxy-*sn*-glycero-3-phosphoethanolamine. However due to the limited solubility of these lipids only HHGP was suitable to conduct the ITC and structural studies. In order to demonstrate the lipid binding property of GrIR is similar to  $\beta$ -

lactoglobulin (a well-known lipocalin structurally homologous to GrIR) we have studied the binding of HHGP with  $\beta$ -lactoglobulin.

### Isothermal Titration Calorimetric studies

Initially ITC experiments were conducted for the three identified lipid molecules to determine the binding affinities. However 1, 2-dioctanoyl-*sn*-glycero-3-phosphate and 1-palmitoyl-2-hydroxy-*sn*-glycero-3-phosphoethanolamine are not completely soluble in Tris-HCl buffer at 20°C, and we were able to obtain an interpretable data only for 1-hexanoyl-2-hydroxy-*sn*-glycero-3-phosphate (HHGP). The results indicated that 1-hexanoyl-2-hydroxy-*sn*-glycero-3-phosphate (HHGP) exhibits a micromolar binding affinity for GrIR and  $\beta$ -lactoglobulin, a closest lipocalin structural homologue of GrIR (Fig. 2). Titrations of GrIR and  $\beta$ -lactoglobulin with HHGP showed negative power deflections indicating an apparent exothermic reaction during the binding. GrIR is a dimer in solution as well as in crystal [1], and two ligand molecules were found to bind to one dimer of GrIR. Likewise,  $\beta$ -lactoglobulin is a homodimeric protein. Therefore, the dimer was considered as the functional unit with two binding sites, and the concentration of protein was employed in a dimer basis (0.015 mM). The calorimetric titrations observed with HHGP binding to both proteins do not correspond to a system with identical binding sites, and nonidentical and/or cooperative binding sites must be assumed. This is another evidence for considering the dimer as the functional entity. Because the protein is a homodimer, with two identical binding sites in the absence of ligand, the two binding sites must exhibit (positive or negative) cooperativity.

Experimental data were analyzed employing a general model based on the overall association constants,  $\beta_i$ , and binding enthalpies,  $\Delta H_i$ , associated with the formation of complex  $ML_i$  [22], from which information on the type of binding sites may be directly inferred (see Supplementary Information).

The non-linear regression analysis indicated that two ligands are binding to a GrIR dimer with  $\beta_1 = (8.4 \pm 0.9) \cdot 10^5 \text{ M}^{-1}$ ,  $\Delta H_1 = -0.1 \pm 0.4 \text{ kcal/mol}$ ,  $\beta_2 = (8.4 \pm 0.7) \cdot 10^{11} \text{ M}^{-1}$ ,  $\Delta H_2 = -7.1 \pm 0.4 \text{ kcal/mol}$ ,  $n = 1.08 \pm 0.06$ . The parameter  $n$  is not the stoichiometry, already accounted for in the model, but the fraction of active protein, as indicated in the Supplementary Information. The cooperativity parameter  $4\beta_2/\beta_1^2$  is equal to 4.7, which indicates that the binding sites exhibit positive cooperativity. Further, the experimental data were analyzed employing a positive cooperativity model with two identical binding sites, using explicitly the microscopic association constant,  $k$ , and binding enthalpy,  $\Delta H$ , for each binding site, and the cooperativity constant,  $\kappa$ , and the cooperativity enthalpy,  $\Delta h$  (see Supplementary Information). The non-linear regression analysis indicated that two ligands are binding to a GrIR dimer with  $k = (4.2 \pm 0.4) \cdot 10^5 \text{ M}^{-1}$ ,  $\Delta H = -0.1 \pm 0.4 \text{ kcal/mol}$ ,  $\kappa = 4.7 \pm 0.3$ ,  $\Delta h = -6.8 \pm 0.4 \text{ kcal/mol}$ ,  $n = 1.08 \pm 0.06$ . These values are identical to the ones calculated directly from the parameters obtained with the general model based on the overall parameters using the appropriate linking equations between the two models (see Supplementary Information).

The non-linear regression analysis also indicated that two ligands are binding to a  $\beta$ -lactoglobulin dimer with  $\beta_1 = (1.4 \pm 0.3) \cdot 10^6 \text{ M}^{-1}$ ,  $\Delta H_1 = -2.2 \pm 0.4 \text{ kcal/mol}$ ,  $\beta_2 = (1.8 \pm 0.4) \cdot 10^{10} \text{ M}^{-1}$ ,  $\Delta H_2 = -13.9 \pm 0.4 \text{ kcal/mol}$ ,  $n = 0.98 \pm 0.08$ . The cooperativity parameter  $4\beta_2/\beta_1^2$  is equal to 0.038, which indicates that the binding sites are non-identical or they exhibit negative cooperativity.  $\beta$ -lactoglobulin is homodimeric, and hence the experimental data were analyzed employing a negative cooperativity model with two identical binding sites using explicitly the microscopic association constant,  $k$ , and binding enthalpy,  $\Delta H$ , for each binding site, and the cooperativity constant,  $\kappa$  and the cooperativity enthalpy,  $\Delta h$  (see Supplementary Information). The non-linear regression analysis indicated that two ligands

are binding to a  $\beta$ -lactoglobulin dimer with  $k = (7.2 \pm 0.9) \cdot 10^5 \text{ M}^{-1}$ ,  $\Delta H = -2.2 \pm 0.4 \text{ kcal/mol}$ ,  $\kappa = 0.038 \pm 0.05$ ,  $\Delta h = -9.5 \pm 0.4 \text{ kcal/mol}$ ,  $n = 0.98 \pm 0.08$ .

The ITC data suggests that each monomer of GrIR interact with one molecule of 1-hexanoyl-2-hydroxy-*sn*-glycero-3-phosphate (HHGP) molecule. We speculate that lipids with two longer hydrocarbon tails may engage simultaneously with the dimeric GrIR, with one tail for each monomer. The highly hydrophobic nature of longer chain lipids prevented us from performing further ITC experiments.

### Structure of GrIR Lipid complex

We attempted to co-crystallize each of the three lipid molecules with GrIR, however, diffraction quality crystals were obtained only for the 1-hexanoyl-2-hydroxy-*sn*-glycero-3-phosphate (HHGP) with GrIR. In our previous study, the lipid binding cavity of GrIR is occupied by a Triton-X100 molecule which was present in the lysis buffer. During the cocrystallization of GrIR with HHGP, we titrated the protein with HHGP using ITC and concentrated the resulting complex for setting up the crystallization screens. Moreover, we did not use any Triton-X100 during the lysis and purification stage. The structure of recombinant GrIR in complex with HHGP was solved by the molecular replacement method using a synchrotron data set and refined to a final R-factor of 0.231 ( $R_{\text{free}}=0.278$ ) at 2.5 Å resolution. There are two GrIR-lipid complex molecules in the asymmetric unit (Fig 3). The simulated annealing omit map (Fig 4) of the bound HHGP molecules shows well defined electron density map. The model has been refined with good stereochemical parameters (Table 1). All the residues of GrIR including the N-terminal linker were well defined in the electron density map, except for the last ten residues at the C-terminus.

The GrIR molecule in the GrIR-HHGP complex is highly similar to that of our previously determined GrIR structure [1]. GrIR is a single domain  $\beta$ -barrel protein. The  $\beta$ -barrel consists of eight anti-parallel  $\beta$ -strands running from one side of the molecule to the other. The inner cavity region of the lipocalins is found to be highly hydrophobic and assumed to be a prerequisite for lipid binding. The diameter of the hydrophobic pore of GrIR is comparable to most of the well known lipocalins (Fig 1B). In the GrIR-HHGP complex there are 30 hydrophobic side chains having extensive hydrophobic interactions with the bound lipid molecule. The ends of the  $\beta$ -barrel are closed off by the N-terminus (Met1 to Lys4) and plug residues Tyr59 to Asp70. This indicates that transport through the hydrophobic cavity is restricted.

Structural comparisons of GrIR with lipocalins revealed an extended loop (L1) (the plug region Tyr59 to Asp70 of GrIR) on one side of the  $\beta$ -barrel, which is significantly longer than other loops (Supplementary Fig 1). This loop may act as a plug to close and open the pore. Several highly conserved hydrophobic residues are located at the middle of this loop. The conformation and nature of this extended loop scaffold (plug region) is similar in all lipocalins. In retinol binding proteins, this loop is shown to be partially responsible for the binding of lipid molecules [8]. The loop (L3) in GrIR, located opposite to the extended loop (plug) has two conserved residues (D17, S18) (Supplementary Fig 1). Similar conserved residues are also observed in PagP (D76 and S77) [23] and MxiM (D124 and T125) structures. These two conserved residues have been reported to be important for the catalytic acyltransferase activity in PagP [23]. Moreover, MxiM has been proposed as a soluble acyltransferase that may act to lipidate components of the T3SS [21]. Similar to the structure of PagP, the loops of GrIR are flexible to accommodate the binding of lipid molecules. A small change in phi-psi angle at both end of the extended loop (L1) may facilitate the opening and closing of the pore, and thus regulate the movement of the lipid molecules through the pore. Considering the high structural similarities of GrIR with PagP and MxiM

and the presence of conserved residues, we speculate that GrIR may also carry an acyltransferase activity.

### Mass spectrometry analysis to identify the physiological lipid species bound to GrIR

In order to establish a physiological role of the lipid binding property and to identify the relevant lipid species, mass spectrometry experiment was carried out. His tagged GrIR was over expressed in bacterial cells and purified using Ni-NTA resins, and was used for lipid extraction. The extracted lipid was analyzed by Q-TOF mass spectrometry to obtain a complete lipid profile of the lipid species that co-purified with GrIR. A representative lipid profile for the GrIR bound species is shown in Fig. 5B. The total cell lipid extract was taken as controls (Fig 5A). In order to discriminate with non-specific bindings, a reference protein, ribosomal modifying methyltransferase (PrmB), which is not reported to bind to any lipids, was also included in the analysis. His-tagged PrmB was over expressed and purified with Ni-NTA. The lipids were extracted from the protein in a similar fashion as that of the GrIR protein. The lipid profile generated from PrmB is shown in Fig 5C. Comparison between the GrIR and the PrmB lipid profile showed drastic differences. Species with the  $m/z$  ratio of 688, 714, 716, 719, 742, 745, 747 and 773 were observed to be significantly higher in the GrIR extracts compared to the PrmB extract. These species were observed to be absent in the Ni-NTA lipid extracts from the un-induced bacterial cultures. Identification of the species was carried out using tandem mass spectrometry. Phosphatidylglycerol and phosphatidylethanolamine species with fatty acid chains of 16:0, 16:1 or 18:1 were observed to be bound to the protein (Fig 6). Interestingly, only specific types of lipid species are observed to be bound to the protein.

A multiple reaction monitoring (MRM) based approach was used to quantify these lipid species in the extracts. In these experiments, the first quadrupole, Q1, is set to pass the precursor lipid ion of interest to the collision cell, Q2, where it underwent collision-induced dissociation. The third quadrupole, Q3, was set to pass the structure specific product ion characteristic of the precursor lipid of interest. MRM is very sensitive and is able to quantify the lipid species with less interference from other lipid species which could also be of the same  $m/z$ . The MRM method was built for the identified lipids and the extracts were used for quantification. As expected, the levels of the identified lipids were observed to be significantly higher in the GrIR extracts as compared to that in the un-induced control and the PrmB extracts (Fig 7). The data obtained from Q-ToF analysis was confirmed with the MRM data which also showed phosphatidylglycerol and phosphatidylethanolamine species with fatty acid chains of 16:0, 16:1 or 18:1 were bound to the protein GrIR.

### Discussion

Structural analysis of GrIR showed that its fold is highly similar to lipocalins or lipid binding proteins. A Triton-X100 molecule was bound in the hydrophobic cavity of the native GrIR. Based on the cavity size and analysis of homologous structures, we predicted that lysophosphosphatidic acid (LPA) can bind to the cavity and subsequently HHGP a representative member of LPAs was chosen for this study. We have co-crystallized the GrIR-HHGP complex and determined its structure. The crystal structure of GrIR with bound lipid ligand showed a dimeric arrangement with a lipid molecule bound to each monomer of the protein. Furthermore, we have performed isothermal calorimetry studies and identified the parameters for the binding of HHGP to GrIR. In addition the binding of HHGP with  $\beta$ -lactoglobulin has been studied and compared with GrIR.

Although GrIR and  $\beta$ -lactoglobulin bind HHGP, according to the data analysis of the ITC experiments the two binding sites in GrIR and  $\beta$ -lactoglobulin dimers show positive and negative cooperativity, respectively. The cooperativity interaction parameter value of 4.7 for

GrIR corresponds to a cooperativity Gibbs energy value  $\Delta g$  of  $-0.9$  kcal/mol, whereas the value of  $0.038$  corresponds to  $+1.9$  cal/mol. The estimated value of the Hill coefficient for GrIR and  $\beta$ -lactoglobulin are  $1.37$  and  $0.33$ , respectively, compared to a value of  $1$  for independent ligand binding.

The intrinsic HHGP binding to GrIR and  $\beta$ -lactoglobulin is characterized by a similar moderate affinity ( $k = (4.2 \pm 0.4) \cdot 10^5 \text{ M}^{-1}$ ,  $k_d = 2.4 \text{ }\mu\text{M}$  for GrIR;  $k = (7.2 \pm 0.4) \cdot 10^5 \text{ M}^{-1}$ ,  $k_d = 1.4 \text{ }\mu\text{M}$  for  $\beta$ -lactoglobulin) with a Gibbs energy of binding of  $-7.5$  kcal/mol and  $-7.9$  kcal/mol, respectively, and it is entropically driven ( $\Delta H = -0.1 \pm 0.4$  kcal/mol,  $-T\Delta S = -7.4 \pm 0.4$  kcal/mol for GrIR;  $\Delta H = -2.2 \pm 0.4$  kcal/mol,  $-T\Delta S = -5.7 \pm 0.4$  kcal/mol for  $\beta$ -lactoglobulin). Therefore, the intrinsic parameters for the binding of HHGP to GrIR and  $\beta$ -lactoglobulin are similar: micromolar binding affinity, small binding enthalpy, and binding dominated by entropy. This is what would be expected for the binding of an apolar molecule: hydrophobic desolvation as the predominating phenomenon, resulting in a remarkable entropy gain and a small enthalpic contribution.

The binding of physiological lipid species with GrIR is further confirmed using mass spectrometric studies which compared the profiles from non-induced and induced bacterial culture. We also identified phosphatidylglycerol (PG) and phosphatidylethanolamine (PE) as the two major lipid species which bound to GrIR. It is well known that PE and PG are the major lipid components of bacterial membranes. The inner membrane of *E. coli* contains 70–80% PE and 20–25% PG [24]. The phosphatidylglycerols and phosphatidic acids differ to some extent in terms of their chemical entities. Phosphatidic acid with a glycerols group becomes phosphatidylglycerol. HHGP which showed micromolar binding affinity in ITC experiment has a head group of phosphatidic acid. Previous studies shows that a major urinary protein (MUP) of mouse (PDB code 1MUP) [25, 26] binds with a number of odorant molecules with varying affinity. A similar multiple binding was also reported in odorant binding protein [27]. Using mass spectrometry experiments we have identified the binding of two different lipid species in GrIR.

Further our ITC experiments with HHGP and  $\beta$ -lactoglobulin demonstrate that HHGP binds to  $\beta$ -lactoglobulin.  $\beta$ -lactoglobulin is a well studied lipocalin and its crystal structures have been reported in complex with palmitic acid (PDB code 1b0o [28]), 12-bromododecanoic acid (PDB code 1bso [29]) and retinol (PDB code 1gx8 [30]). The structural comparison of the  $\beta$ -lactoglobulin-lipid complexes compares well with GrIR-HHGP structure. Moreover, the binding of HHGP with other known lipocalins like blc [10] and Mxim [21] were previously reported. Besides, the co-crystal structure of Mxim with HHGP is similar to GrIR: HHGP complex. HHGP showed micro-molar binding affinity with both GrIR and Mxim [21].

Future studies will be directed towards understanding the relationship, if any, between the regulatory and lipid binding function of GrIR. We speculate that GrIR might be having multiple functions as a regulatory protein as well as lipid binding/transport protein and these functions may be changed according to the physiological condition of the bacteria. In this context it is worth mentioning here that the bacterial outer membrane enzyme PagP was found to transfer a palmitate chain from a phospholipid to lipid A [23]. PagP is a close structural homologue of GrIR, suggesting that GrIR has the potential to carry lipid molecules.

## Supplementary Material

Refer to Web version on PubMed Central for supplementary material.

## Acknowledgments

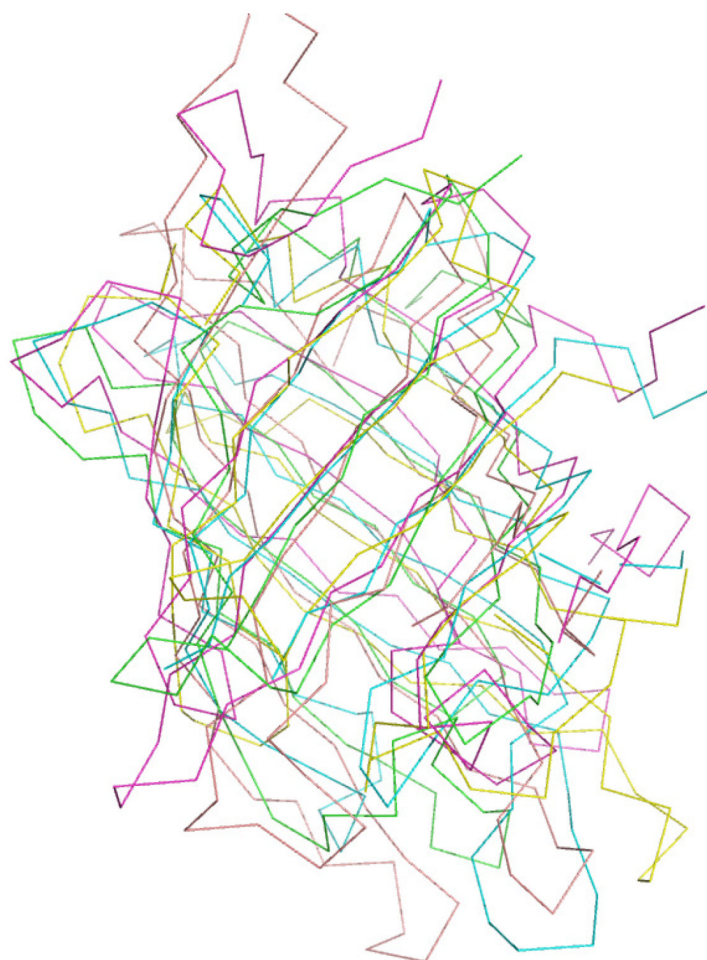
The authors would like to acknowledge X29 beam-line, Brookhaven National Laboratory, NSLS, for the data collection and thank Dr. Anand Saxena for the help during the data collection. We thank Dr Zhou Xingding for the useful discussion. Jobichen Chacko is a graduate scholar in receipt of a research scholarship from NUS.

**Funding.** This work was supported by a BMRC grant from the Agency for Science Technology and Research (A\*STAR), Grant R-154-000-368-305, Singapore. J.S acknowledges the research support from Academic Research Fund (Grant No. R154000254112), National University of Singapore (NUS). M.R.W is supported in part by the Singapore National Research Foundation under CRP Award No. 2007-04, the Academic Research Fund (R-183-000-160-112), the Biomedical Research Council of Singapore (R-183-000-134-305, R-183-000-211-305) and the National Medical Research Council (R-183-000-224-213). A.V.-C. was supported by grant SAF2004-07722 from the Spanish Ministry of Education and Science, a Ramon y Cajal Research Contract from the Spanish Ministry of Science and Technology, and Fundacion Aragon I+D (Diputacion General de Aragon).

## References

1. Jobichen C, Li M, Yerushalmi G, Tan Y, Mok Y, Rosenshine I, Leung K, Sivaraman J. Structure of GrIR and the implication of its EDED motif in mediating the regulation of type III secretion system in EHEC. *PLoS Pathog.* 2007; 3:e69. [PubMed: 17511515]
2. Bishop R, Penfold S, Frost L, Høltje J, Weiner J. Stationary phase expression of a novel *Escherichia coli* outer membrane lipoprotein and its relationship with mammalian apolipoprotein D. Implications for the origin of lipocalins. *J Biol Chem.* 1995; 270:23097–23103. [PubMed: 7559452]
3. Bishop R. The bacterial lipocalins. *Biochim Biophys Acta.* 2000; 1482:73–83. [PubMed: 11058749]
4. Akerstrom B, Flower D, Salier J. Lipocalins: unity in diversity. *Biochim Biophys Acta.* 2000; 1482:1–8. [PubMed: 11058742]
5. Flower D, North A, Sansom C. The lipocalin protein family: structural and sequence overview. *Biochim Biophys Acta.* 2000; 1482:9–24. [PubMed: 11058743]
6. Flower D. Experimentally determined lipocalin structures. *Biochim Biophys Acta.* 2000; 1482:46–56. [PubMed: 11058746]
7. Grzyb J, Latowski D, Strzałka K. Lipocalins – a family portrait. *J Plant Physiol.* 2006; 163:895–915. [PubMed: 16504339]
8. Flower D. Multiple molecular recognition properties of the lipocalin protein family. *J Mol Recognit.* 1995; 8:185–195. [PubMed: 8573354]
9. Flower D, North A, Attwood T. Structure and sequence relationships in the lipocalins and related proteins. *Protein Sci.* 1993; 2:753–761. [PubMed: 7684291]
10. Campanacci V, Nurizzo D, Spinelli S, Valencia C, Tegoni M, Cambillau C. The crystal structure of the *Escherichia coli* lipocalin Blc suggests a possible role in phospholipid binding. *FEBS Lett.* 2004; 562:183–188. [PubMed: 15044022]
11. Flower D. The up-and-down beta-barrel proteins: three of a kind. *FASEB J.* 1995; 9:566–567. [PubMed: 7737467]
12. Matthews B. Solvent content of protein crystals. *J Mol Biol.* 1968; 33:491–497. [PubMed: 5700707]
13. Otwinowski Z, Minor W. Processing of X-ray diffraction data collected in oscillation mode. *Methods Enzymol.* 1997; 276:307–326.
14. McCoy A. Solving structures of protein complexes by molecular replacement with Phaser. *Acta Crystallogr D Biol Crystallogr.* 2007; 63:32–41. [PubMed: 17164524]
15. Collaborative Computational Project, Number 4. *Acta Cryst D.* 1994; 50:760–763. [PubMed: 15299374]
16. Brünger A, Adams P, Clore G, DeLano W, Gros P, Grosse-Kunstleve R, Jiang J, Kuszewski J, Nilges M, Pannu N, Read R, Rice L, Simonson T, Warren G. Crystallography & NMR system: A new software suite for macromolecular structure determination. *Acta Crystallogr D Biol Crystallogr.* 1998; 54:905–921. [PubMed: 9757107]
17. Jones T, Zou J, Cowan S, Kjeldgaard M. Improved methods for building protein models in electron density maps and the location of errors in these models. *Acta Crystallogr A.* 1991; 47(Pt 2):110–119. [PubMed: 2025413]

18. Laskowski R, Moss D, Thornton J. Main-chain bond lengths and bond angles in protein structures. *J Mol Biol.* 1993; 231:1049–1067. [PubMed: 8515464]
19. Holm L, Sander C. Mapping the protein universe. *Science.* 1996; 273:595–603. [PubMed: 8662544]
20. Altschul S, Madden T, Schäffer A, Zhang J, Zhang Z, Miller W, Lipman D. Gapped BLAST and PSI-BLAST: a new generation of protein database search programs. *Nucleic Acids Res.* 1997; 25:3389–3402. [PubMed: 9254694]
21. Lario P, Pfuetzner R, Frey E, Creagh L, Haynes C, Maurelli A, Strynadka N. Structure and biochemical analysis of a secretin pilot protein. *EMBO J.* 2005; 24:1111–1121. [PubMed: 15775974]
22. Wyman, J.; Gill, S. *Binding and Linkage Functional Chemistry of Biological Macromolecules.* University Science Books; Mill Valley, California: 1990.
23. Hwang P, Choy W, Lo E, Chen L, Forman-Kay J, Raetz C, Privé G, Bishop R, Kay L. Solution structure and dynamics of the outer membrane enzyme PagP by NMR. *Proc Natl Acad Sci USA.* 2002; 99:13560–13565. [PubMed: 12357033]
24. Dowhan W. Molecular basis for membrane phospholipid diversity: why are there so many lipids? *Annu Rev Biochem.* 1997; 66:199–232. [PubMed: 9242906]
25. Böcskei Z, Groom C, Flower D, Wright C, Phillips S, Cavaggioni A, Findlay J, North A. Pheromone binding to two rodent urinary proteins revealed by X-ray crystallography. *Nature.* 1992; 360:186–188. [PubMed: 1279439]
26. Cavaggioni A, Findlay J, Tirindelli R. Ligand binding characteristics of homologous rat and mouse urinary proteins and pyrazine-binding protein of calf. *Comp Biochem Physiol B.* 1990; 96:513–520. [PubMed: 2390861]
27. Monaco H, Zanotti G. Three-dimensional structure and active site of three hydrophobic molecule-binding proteins with significant amino acid sequence similarity. *Biopolymers.* 1992; 32:457–465. [PubMed: 1623143]
28. Wu SY, Perez MD, Puyol P, Sawyer L. beta-lactoglobulin binds palmitate within its central cavity. *J Biol Chem.* 1999; 274:170–174. [PubMed: 9867826]
29. Qin BY, Creamer LK, Baker EN, Jameson GB. 12-Bromododecanoic acid binds inside the calyx of bovine beta-lactoglobulin. *FEBS Lett.* 1998; 438:272–278. [PubMed: 9827560]
30. Kontopidis G, Holt C, Sawyer L. The ligand-binding site of bovine beta-lactoglobulin: evidence for a function? *J Mol Biol.* 2002; 318:1043–1055. [PubMed: 12054801]
31. DeLano, WL. The PyMOL molecular graphics system. 2002. Available : [www.pymol.org](http://www.pymol.org)
32. Larkin M, Blackshields G, Brown N, Chenna R, McGettigan P, McWilliam H, Valentin F, Wallace I, Wilm A, Lopez R, Thompson J, Gibson T, Higgins D. Clustal W and Clustal X version 2.0. *Bioinformatics.* 2007; 23:2947–2948. [PubMed: 17846036]
33. Gouet P, Courcelle E, Stuart D, Métoz F. ESPript: analysis of multiple sequence alignments in PostScript. *Bioinformatics.* 1999; 15:305–308. [PubMed: 10320398]
34. Freire E, Schön A, Velazquez-Campoy A. Isothermal titration calorimetry: General formalism using binding polynomials. *Methods Enzymol.* 2009 in press.
35. Velazquez-Campoy A, Freire E. ITC in the post-genomic era...? *Priceless Biophys Chem.* 2005; 115:115–124.



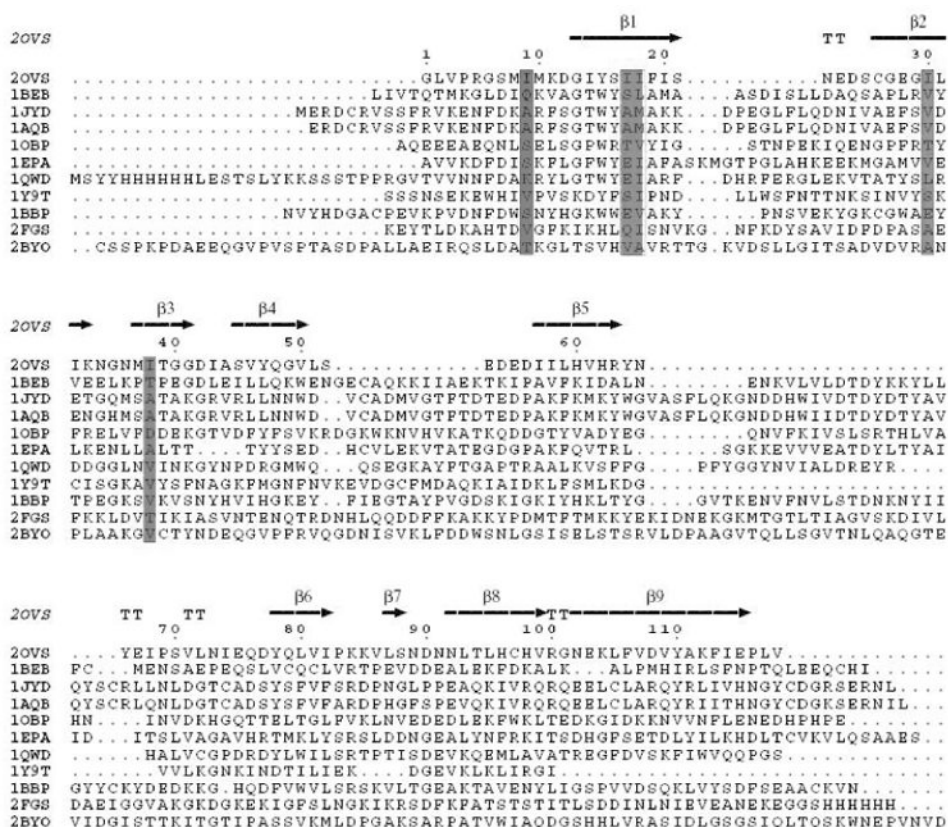


**Fig. 1.**

**A.** Superposition of GrlR with major lipocalins. GrlR - green, Retinol binding protein (PDB code 1JYD) - blue, Major Urinary protein (pdb code 1MUP) - violet, Outer membrane lipoprotein blc (PDB code 1QWD) - yellow, Outer membrane enzyme pagp (PDB code 1THQ)-brown. This figure was prepared using Pymol software [31].

**B.** Sequence alignment of GrlR with major lipocalins. Pdb codes - 20vs: GrlR, 1beb: bovine  $\beta$ -lactoglobulin, 1jyd: human serum retinol-binding protein, 1aqb: pig plasma retinol-binding protein, 1obp: bovine odorant binding protein, 1epa: epididymal retinoic acid binding protein, 1qwd: blc, 1y9t: Mxim, 1bbp: bilin binding protein, 2fgs: Campylobacter Jejuni YceI Periplasmic Protein, 2byo: LppX (<http://www.rcsb.org>). The alignment was performed using ClustalW [32] and the figure was prepared using Esript [33].

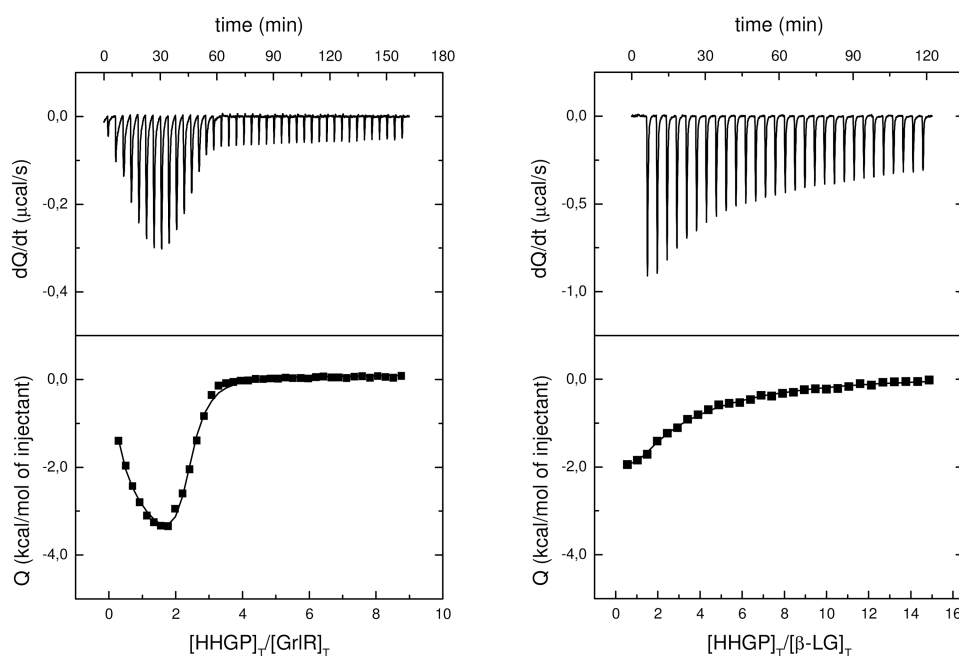


**Fig 2.**

ITC data for the titration of (Left) 0.9 mM hexanoyl-2-hydroxy-*sn*-glycero-3-phosphate (HHGP) into 0.015 mM GrIR, and (Right) 1.0 mM hexanoyl-2-hydroxy-*sn*-glycero-3-phosphate (HHGP) into 0.015 mM  $\beta$ -lactoglobulin. The upper panels contain the baseline-corrected raw data, and the lower panels show the peak-integrated, concentration normalized heats of reaction versus the molar ratio. The solid line in the lower panels represents the best fit of the data using the general model using the overall binding constants for two binding sites, or the model with two identical binding sites with positive (GrIR) or negative cooperativity ( $\beta$ -lactoglobulin).

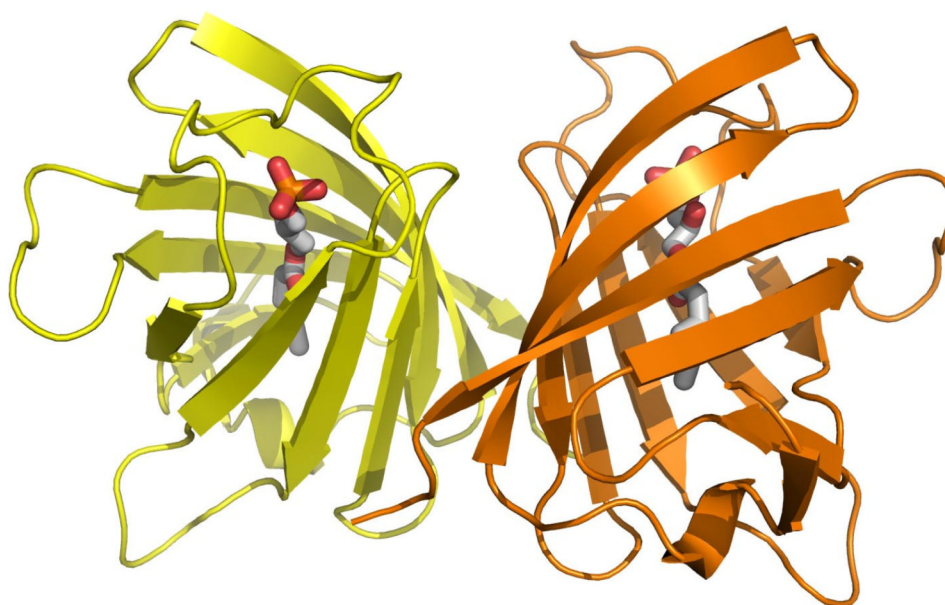


**Fig 3.** Overall structure of GrIR with bound 1-hexanoyl-2-hydroxy-*sn*-glycero-3-phosphate (HHGP). Ribbon diagram of dimeric GrIR and bound HHGP is shown in stick model. The C-terminal 11 residues are disordered and were not included in this structure. This figure was prepared using Pymol [31].

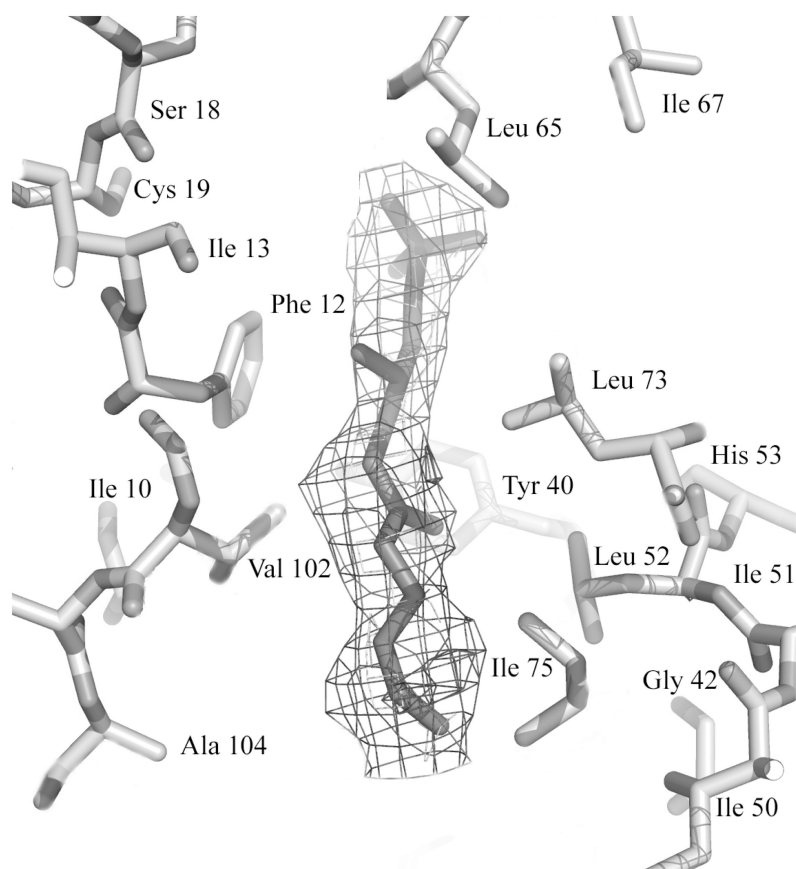


**Fig. 4.** Simulated annealing Fo-Fc omit map in the pore region of GrIR. The bound hexanoyl-2-hydroxy-*sn*-glycero-3-phosphate (lipid) molecule and all atoms within 2 Å of the lipid molecule were omitted prior to refinement. The map contoured at a level of  $3\sigma$ . This figure was prepared using Pymol [31].

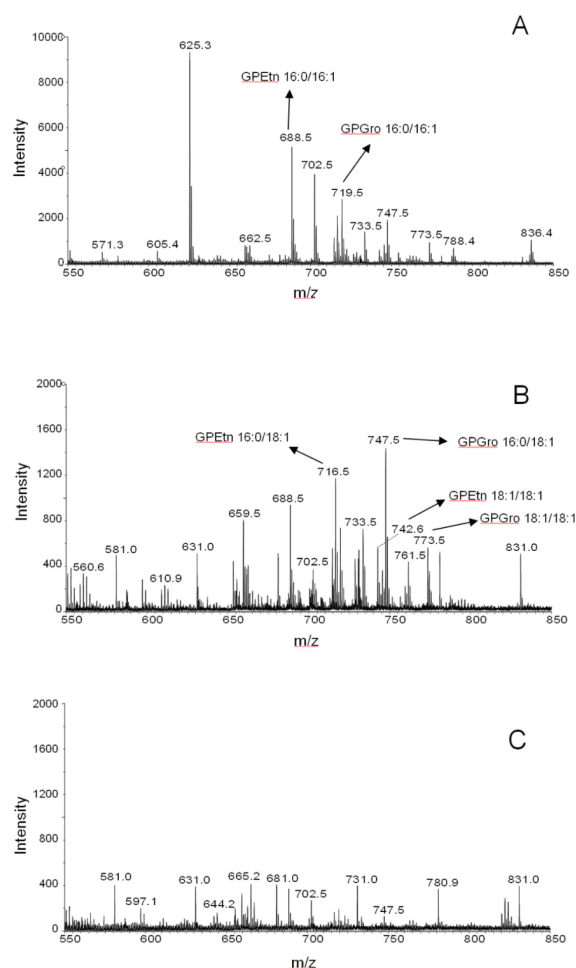
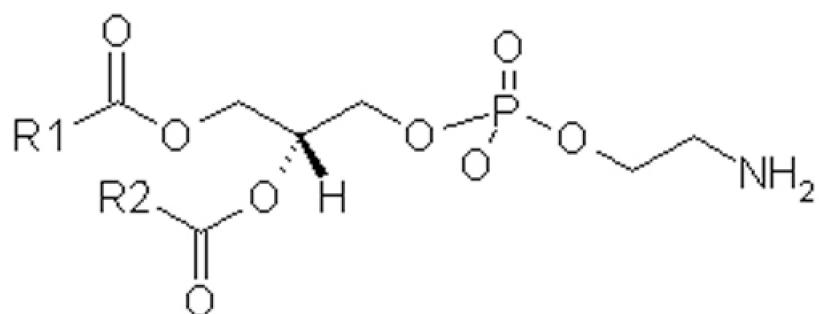
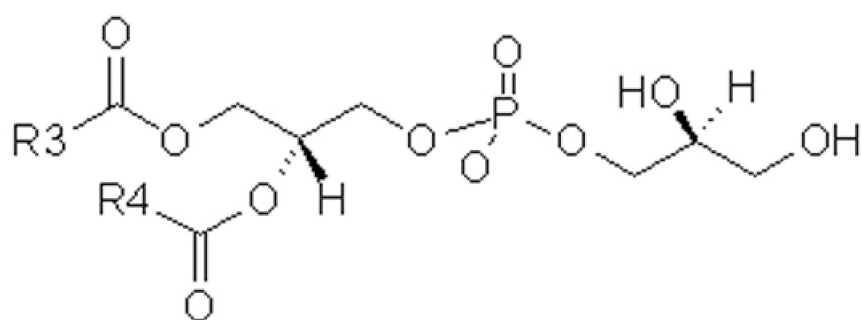


**Fig 5. Lipid profile using mass spectrometry**

The lipid were extracted from (A) GrlR over-expressed cells (B) Ni-NTA extracts from GrlR over-expressed cells and (C) Ni-NTA extracts from methyl transferase over-expressed cells. The data is the representative profile of 3 different set of experiments.



Phosphatidylethanolamine



Phosphatidylglycerol

**Fig 6.** Basic structure of phosphatidylglycerol and phosphatidylethanolamine. R1, R2, R3 and R4 indicates the fatty acids

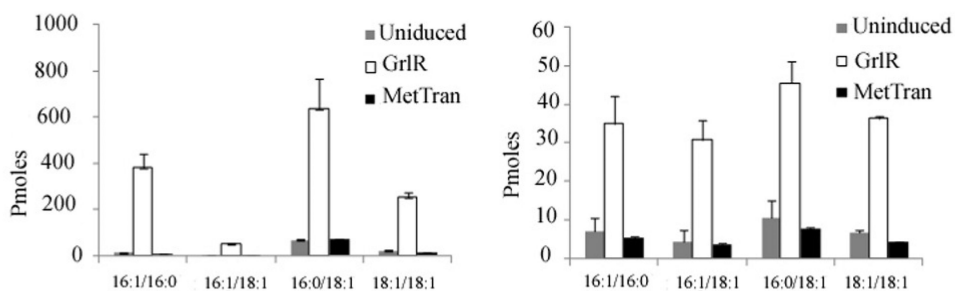


**Fig 7. MRM based quantification of lipids**

The Ni-NTA lipid extracts from the uninduced (grey box), GrIR over expressed (open box) and the methyl transferase over expressed (black box) cells were passed through a MRM based quantification for phosphatidylglycerol and phosphatidylethanolamine. The number below the bars indicates the fatty acid composition of the respective lipid class. The data is from 3 replicates and is the representative of 3 different sets of experiments.

**Table 1**  
**Data collection and refinement statistics**

Data collection	High resolution
Space group	P2 <sub>1</sub> 2 <sub>1</sub> 2 <sub>1</sub>
Cell dimensions	
<i>a</i> , <i>b</i> , <i>c</i> (Å)	43.73, 66.02, 83.46
$\alpha$ , $\beta$ , $\gamma$ (°)	90, 90, 90
Resolution (Å)	2.5
$aR_{\text{sym}}$	10.3
<i>I</i> / $\sigma I$	8.2
Completeness (%)	98.9
Redundancy	6.7
<b>Refinement</b>	
Resolution (Å)	20- 2.5
No. reflections	8751
$bR_{\text{work}}/^cR_{\text{free}}$	0.231 / 0.278
<b>Number of atoms</b>	
Protein	1836
Ligand/ion	34
Water	264
<b>B-factors</b>	
Protein	34.256
Ligand/ion	36.48
Water	51.869
<b>R.m.s deviations</b>	
Bond lengths (Å)	0.01
Bond angles (°)	1.7
<b>Ramachandran Plot</b>	
Most favorable regions (%)	84.2
Additional allowed regions (%)	13.9
Generously allowed regions (%)	2.0
Disallowed regions (%)	0

<sup>a</sup> $R_{\text{sym}} = \sum |I_i - \langle I \rangle| / \sum |I_i|$  where  $I_i$  is the intensity of the  $i^{\text{th}}$  measurement, and  $\langle I \rangle$  is the mean intensity for that reflection.

<sup>b</sup> $R_{\text{work}} = \sum |F_{\text{obs}} - F_{\text{calc}}| / \sum |F_{\text{obs}}|$  where  $F_{\text{calc}}$  and  $F_{\text{obs}}$  are the calculated and observed structure factor amplitudes, respectively.

<sup>c</sup> $R_{\text{free}}$  = as for  $R_{\text{work}}$ , but for 5.0% of the total reflections chosen at random and omitted from refinement.